Research Square

Preprints are preliminary reports that have not undergone peer review.
They should not be considered conclusive, used to inform clinical practice,
or referenced by the media as validated information.

Integrated Fermentation: Distillation and Thermodynamic Assessment of Ethanol Production from Tropical Biomass (Pineapple, Dragon Fruit, and Cupuaçu)

Mayra Kerolly Sales Monteiro

mayra.monteiro@ifro.edu.br

Federal Institute of Education, Science and Technology of Rondônia, IFRO

Valdivino Francisco dos Santos Borges

Federal Institute of Education, Science and Technology of Rondônia, IFRO

Rafael Vieira

Federal Institute of Education, Science and Technology of Rondônia, IFRO

João Miller Melo Henrique

Federal Institute of Sertão Pernambucano

Elisama Vieira Santos

Federal University of Rio Grande do Norte

Carlos A. Martínez-Huitle

Federal University of Rio Grande do Norte

Research Article

Keywords: Bioethanol production, Tropical biomass valorization, Fractional distillation, Liquid–vapor equilibrium (LVE), McCabe-Thiele analysis

Posted Date: August 26th, 2026

DOI: https://doi.org/10.21203/rs.3.rs-8904561/v1

License: This work is licensed under a Creative Commons Attribution 4.0 International License.
Read Full License

Additional Declarations: No competing interests reported.

Integrated Fermentation: Distillation and Thermodynamic Assessment of Ethanol Production from Tropical Biomass (Pineapple, Dragon Fruit, and Cupuaçu)

Mayra Kerolly Sales Monteiro[1], Valdivino Francisco dos Santos Borges[1], Rafael Vieira[1], João Miller Melo Henrique[2], Elisama Vieira dos Santos[3], Carlos A. Martínez-Huitle[3]

[1] Federal Institute of Education, Science and Technology of Rondônia, IFRO, Rua Rio Amazonas, n° 151 – Jardim dos Migrantes, 76900-730, Brazil.
[2] Federal Institute of Sertão Pernambucano, IFSertãoPE, Estrada do Tamboril, s/n - Vila Quixada, CEP 56.200-000, Ouricuri-PE, Brazil.
[3]Renewable Energies and Environmental Sustainability Research Group, Institute of Chemistry, Federal University of Rio Grande do Norte, Campus Universitário, Av. Salgado Filho 3000, Lagoa Nova, Natal CEP 59078-970, RN, Brazil.
email:mayra.monteiro@ifro.edu.br

Abstract

The increasing demand for renewable biofuels has intensified the search for alternative feedstocks and sustainable technological routes for ethanol production, particularly from tropical biomass and agro-industrial residues. In this context, pineapple (Ananas comosus), dragon fruit (Hylocereus spp.), and cupuaçu (Theobroma grandiflorum) present significant fermentable potential but remain insufficiently explored through integrated thermodynamic and process engineering approaches. This study evaluates ethanol production from these tropical matrices via alcoholic fermentation using Saccharomyces cerevisiae, followed by differential and fractional distillation, liquid–vapor equilibrium (LVE) modeling, McCabe–Thiele analysis, and pilot-scale process simulation. Pineapple exhibited the highest initial sugar content (~13 g/100 g), followed by dragon fruit (~9 g/100 g) and cupuaçu (~6.5 g/100 g), directly influencing ethanol productivity. Fermentation yields ranged from 76–85% of theoretical ethanol, consistent with complex biomass systems. Fractional distillation significantly outperformed differential distillation, achieving higher ethanol enrichment, reduced water entrainment, and closer agreement with LVE predictions. McCabe–Thiele diagrams indicated an increase in effective theoretical stages from approximately one (differential) to 4–6 (fractional), demonstrating the critical role of reflux in separation efficiency. Process simulation highlighted the importance of must standardization, adequate reflux ratio, and thermal integration for industrial feasibility. Overall, the results confirm the technical

potential of tropical fruits – particularly pineapple – as sustainable feedstocks for ethanol production within circular bioeconomy frameworks.

Keywords: Bioethanol production; Tropical biomass valorization; Fractional distillation; Liquid–vapor equilibrium (LVE); McCabe-Thiele analysis

1. Introduction

The transition toward renewable energy systems has intensified global efforts to develop sustainable pathways for liquid biofuel production, particularly ethanol, which is widely employed as both a transportation fuel and a strategic platform molecule for the chemical, pharmaceutical, and materials industries. Although first-generation ethanol production from conventional feedstocks such as sugarcane and corn is technologically consolidated, increasing environmental concerns, land-use competition, and the need for regional diversification of biomass resources have stimulated the search for alternative substrates. In tropical regions, where biodiversity and fruit production are abundant, the valorization of fruit biomass and agro-industrial residues represents a promising strategy within circular bioeconomy frameworks (Dias, M. O. S. et al., 2012; Balat, M. & Balat, H., 2009).

Tropical fruits such as pineapple (Ananas comosus), dragon fruit (Hylocereus spp.), and cupuaçu (Theobroma grandiflorum) contain significant concentrations of fermentable sugars and exhibit distinct physicochemical compositions that directly influence fermentation kinetics, ethanol productivity, and downstream separation performance. Despite their potential, most reported studies focus primarily on fermentation efficiency or ethanol quantification, often neglecting the integration between biochemical conversion and thermodynamic separation behavior (Kim & Dale, 2004). However, ethanol recovery and purity are not governed solely by fermentative yield; they are strongly dependent on the efficiency of the distillation system and on the liquid–vapor equilibrium (LVE) characteristics of the ethanol–water mixture (Gnansounou & Dauriat, 2010).

Distillation remains the dominant industrial technology for ethanol purification, accounting for a substantial fraction of total process energy consumption. The separation performance depends fundamentally on the number of equilibrium stages, reflux ratio, vapor–liquid contact efficiency, and thermal control. Differential distillation, which

operates without reflux and approximates a single equilibrium stage, is inherently limited in enrichment capacity (Kiss, A. A.; et al., 2013; Luyben, W. L., 2011). In contrast, fractional distillation introduces internal reflux, enabling multiple theoretical stages and substantially improving separation efficiency. Classical thermodynamic tools such as T–x–y diagrams and the McCabe–Thiele method provide a quantitative framework to interpret these differences, allowing direct estimation of theoretical stage numbers and evaluation of deviations from ideal equilibrium behavior (Towler & Sinnot, 2013).

Moreover, the integration of mass balance modeling with experimental LVE data enables a more rigorous understanding of how feed composition, separation strategy, and operating conditions interact to determine global process efficiency (Biegler, L. T. et al., 1997). When combined with pilot-scale flowsheet simulation, such analyses allow laboratory-scale findings to be extrapolated to industrial scenarios, highlighting the importance of must standardization, reflux optimization, column design, and heat integration for economic feasibility (Cardona & Sánchez, 2007; YAWS, C. L., 2008).

In this context, the present study proposes an integrated assessment of ethanol production from tropical biomass matrices – pineapple, dragon fruit, and cupuaçu - combining alcoholic fermentation using Saccharomyces cerevisiae, differential and fractional distillation, analytical characterization, thermodynamic LVE analysis, McCabe-Thiele graphical evaluation, and pilot-scale process simulation. By correlating initial sugar content, fermentation performance, separation efficiency, and thermodynamic behavior, this work provides a comprehensive framework for evaluating the technical feasibility of ethanol production from tropical fruits, contributing to the development of sustainable biofuel pathways aligned with circular economy principles and process engineering optimization.

2. Materials and Methods

2.1 Raw materials

Carbohydrate-rich tropical biomass matrices were used as substrates, including pineapple (Ananas comosus), dragon fruit (Hylocereus spp.), and cupuaçu (Theobroma grandiflorum). All fruits were selected at appropriate ripening stages to ensure high fermentable sugar content and processed immediately after acquisition to minimize

compositional degradation. Commercial biological yeast containing Saccharomyces cerevisiae was employed as the fermentative microorganism.

2.2 Fermentation Procedure

The fermentation process was initiated by preparing a sugar-rich must from fully ripe fruits. After washing and sanitization, the fruits were crushed integrally (pulp and peel) and homogenized with minimal water addition to preserve fermentable sugar concentration. The yeast (Saccharomyces cerevisiae, 5 g) was rehydrated in warm water (35–38 °C) prior to inoculation. The reactivated yeast was then introduced into the must, which was transferred to a fermentation vessel equipped with a hydraulic airlock to ensure anaerobic conditions while allowing CO_2 release. Approximately 20% headspace was maintained to prevent pressure buildup. Fermentation was conducted at ambient temperature (20–30 °C) for 72 h with gentle daily agitation to enhance mass transfer and substrate homogenization. Under anaerobic conditions, fermentable sugars (primarily glucose, fructose, and hydrolyzed sucrose) were metabolized into ethanol and carbon dioxide according to classical yeast fermentation pathways. At the end of fermentation, the medium was clarified by sieving and filtration through filter paper to remove suspended solids, yielding a clear fermented broth suitable for subsequent distillation and analytical characterization (Walker & Stewart, 2016).

2.3 Determination of Reducing Sugars

Reducing sugars were quantified using the Lane–Eynon redox titration method with Fehling's solutions A and B under alkaline conditions. Initially, the Fehling solution was standardized using a glucose standard solution to determine the equivalence factor between reducing sugar concentration and titrant volume. Fruit samples were appropriately diluted and filtered when necessary to ensure titration volumes fell within the method's operational range. Titration was conducted under mild boiling conditions with methylene blue as a redox indicator. The endpoint was defined by the persistent disappearance of the blue coloration, indicating complete reduction of Cu(II) to Cu(I) with formation of cuprous oxide. Reducing sugar content was expressed as glucose equivalents, considering the Fehling factor, titrated volumes, and dilution factors applied (Nielsen, 2017).

2.4 Ethanol Distillation Procedures

2.4.1 Differential Distillation

Differential distillation was employed as the initial ethanol separation step, operating at atmospheric pressure without reflux. After clarification, the fermented ethanol–water mixture was subjected to controlled heating in a simple distillation apparatus. Temperature was continuously monitored from the first to the last drop of distillate. The system was heated to approximately 78 °C, corresponding to the boiling point of ethanol-rich mixtures. Distillate fractions were collected sequentially at defined volume intervals. The density of each fraction was measured, allowing estimation of ethanol concentration throughout the process. Because no reflux was applied, the liquid composition in the boiler continuously changed over time, consistent with the mass balance framework for differential distillation described by the Rayleigh equation (Seader et al., 2011).

2.4.2 Fractional Distillation

Subsequently, fractional distillation was performed to enhance separation efficiency and ethanol purity. A fractionating column was incorporated into the system, allowing partial condensation and internal reflux. During operation, temperature, collected distillate volume, and density were simultaneously monitored. The presence of reflux promoted repeated vapor–liquid contact, increasing effective equilibrium stages and enriching the distillate in ethanol. The experimental data obtained enabled direct comparison with differential distillation and allowed construction of composition–temperature relationships (x–y–T) (Seader et al., 2011).

2.5 Distillation Modeling and Mass Balance Analysis

Distillation modeling was developed based on total and component mass balances for the binary ethanol–water system, considering two cases: Differential distillation (without reflux) and Differential distillation with fractionation (with reflux). The derivations were based on classical assumptions: Perfect mixing in the boiler; Instantaneous vapor–liquid equilibrium; Quasi-steady operation; Binary mixture behavior (Smith, 1963).

2.5.1 Differential distillation (without reflux)

Let L be the mass of liquid remaining in the boiler at a given instant and x the mass fraction of ethanol in that liquid. The differential mass of vapor removed from the system is represented by dV, containing a mass fraction y of ethanol. Since there is no reflux, all the vapor generated is removed as distillate, so that:

$$dV = -dL \quad (1)$$

The mass balance of ethanol in the boiler can be written as:

$$(x - dx)(L - dL) = xL - y\,dV \quad (2)$$

Expanding Equation (2) and neglecting second-order terms (dx·dL), we obtain:

$$-x\,dL - L\,dx = -y\,dV \quad (3)$$

Substituting the relationship given by Equation (1) into Equation (3), we get:

$$-x\,dL - L\,dx = y\,dL \quad (4)$$

Reorganizing the terms:

$$-L\,dx = (y - x)\,dL \quad (5)$$

Separating the variables and integrating between the initial (L_0, x_0) and final (W, xW) conditions:

$$\int_{L_0}^{W} \frac{dL}{L} = \int_{x_0}^{xW} \frac{dX}{(y-x)} \quad (6)$$

Equation (6) corresponds to the Rayleigh equation for differential distillation, with the relation y = f(x) obtained from the liquid-vapor equilibrium of the ethanol-water system.

2.5.2 Differential distillation with fractionation (with reflux)

In the case of fractional distillation, the presence of reflux is considered, defined by the reflux ratio r, given by:

$$r = L' / V \quad (7)$$

where L′ represents the mass flow rate of liquid returning to the column as reflux and V the mass flow rate of ascending vapor. For a differential step, we have:

$$dL' = r\,dV \quad (8)$$

The change in the mass of liquid in the boiler becomes:

$$dL = dL' - dV \quad (9)$$

Substituting Equation (8) into Equation (9):

$$dL = (r - 1)\, dV \quad (10)$$

The differential mass balance of ethanol in the boiler, considering now the reflux inlet and the steam outlet, can be expressed as:

$$(x - dx)(L - dL) = xL + x\, dL' - y\, dV \quad (11)$$

Expanding Equation (11) and neglecting second-order terms:

$$-x\, dL - L\, dx = x\, dL' - y\, dV \quad (12)$$

Substituting Equations (8) and (10) into Equation (12) and rearranging the terms, we obtain:

$$(y + (1 - 2r)x)\, dL = (r - 1)\, L\, dx \quad (13)$$

Separating the variables and integrating between the initial and final states:

$$\int_{L_0}^{W} \frac{dL}{L} = \int_{x_0}^{xW} \left[\frac{(r-1)\, dx}{y + (1 - 2r)x}\right] \quad (14)$$

Equation (14) represents the integrated form of the mass balance for differential distillation with fractionation, explicitly showing the influence of the reflux ratio on the enrichment of the distillate in ethanol.

In both cases, the overall mass and component balances are used to close the system:

$$L_0 = D + W \quad (15)$$

$$x_0 L_0 = xD^*D + xW^*W \quad (16)$$

where D is the total mass of distillate collected and W is the mass of final residue in the boiler.

2.6 Analytical Characterization of Ethanol

Ethanol concentration was determined by UV–Vis spectrophotometry using an indirect dichromate oxidation method. In acidic medium, ethanol reacts with potassium dichromate ($K_2Cr_2O_7$), reducing Cr(VI) to Cr(III), which produces a green coloration measurable at 575 nm (Caputi et al., 1968).Calibration curves were prepared using ethanol standard solutions at known concentrations, and linear regression was applied according to the Beer–Lambert law. Samples were diluted when necessary and subjected to identical chemical treatment as the standards. Ethanol concentration was calculated from the calibration equation, and analytical reliability was evaluated through determination of linearity (R^2), repeatability, and consistency with density measurements.

Density measurements were performed by pycnometry at 20 °C and used as an independent method to assess ethanol–water mixture composition.

2.7 Process Simulation

Process simulation was performed using COCO Simulator (CAPE-OPEN steady-state environment) to represent a pilot-scale ethanol purification system fed with a binary ethanol–water stream equivalent to the experimentally fermented must. The thermodynamic behavior of the mixture was modeled using the Non-Random Two-Liquid (NRTL) activity coefficient model, which is suitable for highly non-ideal polar systems such as ethanol–water. Vapor–liquid equilibrium (VLE) calculations were performed under atmospheric pressure (101.3 kPa), assuming γ–φ formulation, where liquid-phase non-ideality was described by NRTL and vapor-phase behavior was considered ideal. The flowsheet included a feed conditioning unit, preheater, fractionated distillation column with defined reflux ratio, total condenser, kettle reboiler, and heat exchanger network. Mass and energy balances were solved under steady-state conditions with convergence based on component flow and temperature tolerance below 10^{-6}. The simulation aimed to evaluate ethanol recovery, stage performance, reflux influence, and potential heat integration strategies, allowing extrapolation of laboratory-scale results to an industrial scenario.

3. Results and Discussion

3.1 Initial Sugar Content and Fermentative Potential of Tropical Matrices

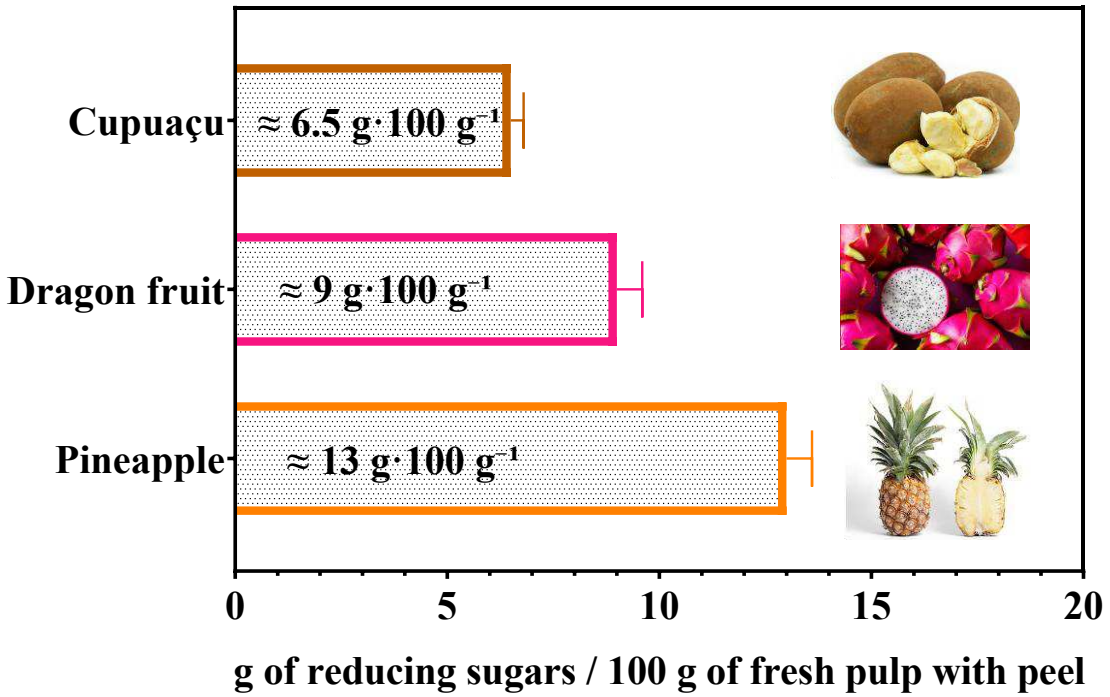


Figure 1: Reducing sugar content (g/100 g) in pineapple, pitaya, and cupuaçu matrices, determined by the Lane–Eynon method, highlighting the initial fermentable potential of each fruit for ethanol production.

Figure 1 quantifies the reducing sugar content of pineapple, dragon fruit, and cupuaçu, revealing marked compositional differences that directly determine their theoretical ethanol production capacity. Pineapple exhibited the highest sugar concentration (≈13 g/100 g), followed by dragon fruit (≈9 g/100 g) and cupuaçu (≈6.5 g/100 g). These differences reflect intrinsic physiological characteristics and ripening profiles, as sugar accumulation in tropical fruits results from starch hydrolysis and sucrose metabolism during maturation (Ramsaroop & Saunders, 2012).

Based on the stoichiometry of alcoholic fermentation:

$$C_6H_{12}O_6 \xrightarrow{Saccharomyces\ cerevisiae\ (anaerobic)} 2C_2H_5OH + 2CO_2 + energy \quad \text{(Eq. 1)}$$

the maximum theoretical ethanol yield corresponds to 0.511 g ethanol per gram of fermentable sugar. Therefore, the higher sugar content measured for pineapple implies a proportionally greater theoretical ethanol production per unit mass of biomass, which directly influences the ethanol concentration in the fermented must. From a process engineering perspective, this initial compositional difference is critical. A must with

higher ethanol concentration reduces the relative energy demand in downstream distillation due to lower water evaporation requirements (Wu, L. et al., 2012). Consequently, Figure 1 not only establishes the biochemical fermentative potential of each matrix but also anticipates differences in separation efficiency and thermal load observed in subsequent stages.

3.2 Fermentation Yield and Global Process Efficiency

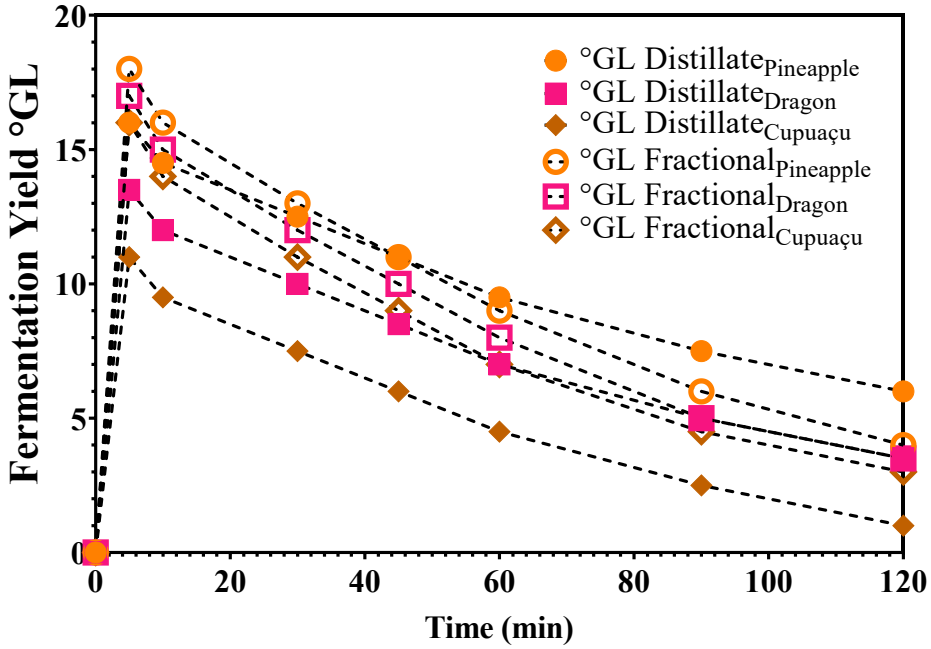


Figure 2: Yield of alcoholic fermentation of pineapple, dragon and cupuaçu matrices, expressed as the ratio between the ethanol recovered experimentally after distillation and the theoretical ethanol estimated from the initial sugar content of the must.

Figure 2 and Table 1 present the relationship between theoretical ethanol production and experimentally recovered ethanol after distillation. Fermentation efficiencies ranged from approximately 76–85% of theoretical yield for most cases, consistent with reported values for complex natural substrates. Deviations from 100% theoretical yield are expected due to: Carbon diversion toward biomass synthesis; Formation of by-products (glycerol, organic acids); Incomplete sugar conversion; Ethanol losses during handling and separation (Cortez, L. A. B. et al., 2008).

For pineapple, despite its higher theoretical ethanol potential (25.26 mL), recovery remained approximately 76%, indicating that biochemical limitations and separation

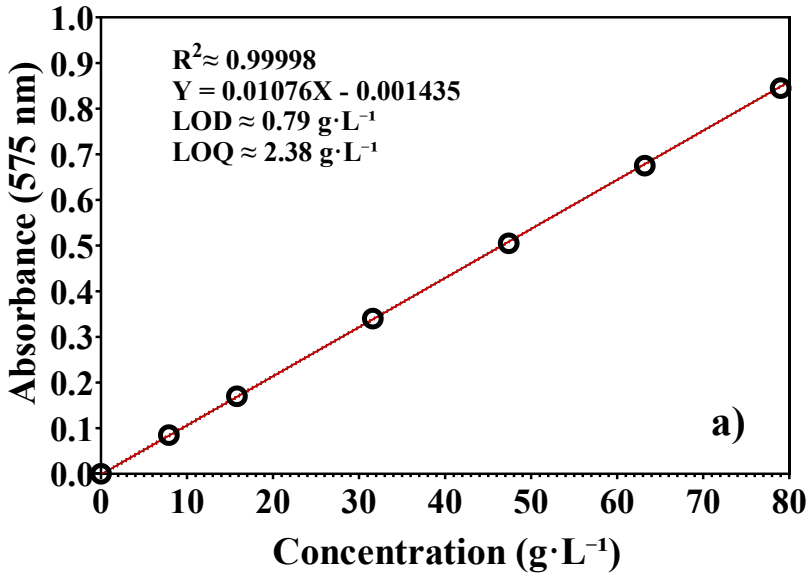
losses influenced the global yield. Dragon fruit showed improved recovery under fractional distillation (≈100.8%), while cupuaçu exhibited apparent recoveries exceeding 100% under fractionation (127.7%). These values do not indicate ethanol overproduction but rather reflect experimental uncertainties in volumetric estimation, density-based calculations, and preferential ethanol enrichment during reflux (Mussatto, S. I. et al., 2010; Bai, F. W. et al., 2008).

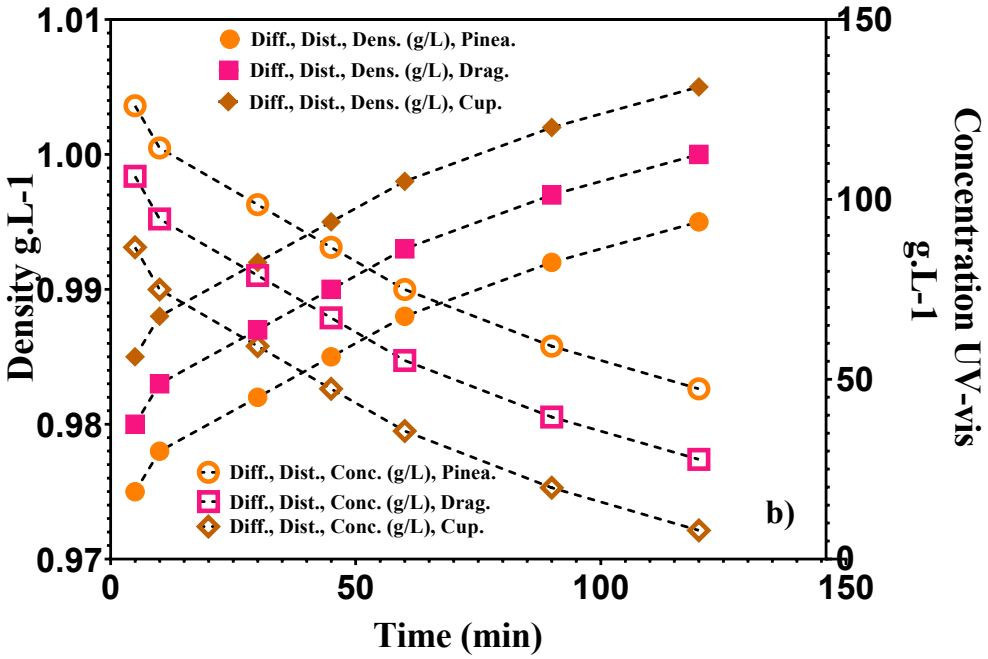
Importantly, the results demonstrate that global efficiency is not governed solely by fermentation performance but by the integration of fermentation and separation strategy.

Table 1: Initial sugar content of pineapple, pitaya, and cupuaçu matrices, estimate of theoretical ethanol produced by fermentation, and comparison with the ethanol effectively recovered in differential and fractional distillations, indicating the overall efficiency of the fermentation and separation process.

Fruit	**Sugar (g/100g)**	**Sugar in the must (g)**	**Theoretical ethanol (g)**	**Theoretical ethanol (mL)**	**Theoretical ethanol in must (% v/v)**
Pineapple	13	39	19.929	25.26	8.42
Dragon	9	27	13.797	17.49	5.83
Cupuaçu	6.5	19.5	9.9645	12.63	4.21
Fruit	**Distillation**	**Ethanol recovered (mL)**	**Ethanol recovered (g)**	**Theoretical ethanol (mL)**	**Recovery vs. theoretical (%)**
Pineapple	Differential	19.25	15.19	25.26	76.2
Pineapple	Fractional	19.25	15.19	25.26	76.2
Dragon	Differential	14.87	11.74	17.49	85
Dragon	Fractional	17.62	13.91	17.49	100.8
Cupuaçu	Differential	10.5	8.28	12.63	83.1
Cupuaçu	Fractional	16.12	12.72	12.63	127.7

3.3 Comparative Analysis of Differential and Fractional Distillation


R²≈ 0.99998
Y = 0.01076X - 0.001435
LOD ≈ 0.79 g·L⁻¹
LOQ ≈ 2.38 g·L⁻¹
a)
Absorbance (575 nm)
Concentration (g·L⁻¹)
0.0
0.1
0.2
0.3
0.4
0.5
0.6
0.7
0.8
0.9
1.0
0
10
20
30
40
50
60
70
80


Diff., Dist., Dens. (g/L), Pinea.
Diff., Dist., Dens. (g/L), Drag.
Diff., Dist., Dens. (g/L), Cup.
Diff., Dist., Conc. (g/L), Pinea.
Diff., Dist., Conc. (g/L), Drag.
Diff., Dist., Conc. (g/L), Cup.
b)
Density g.L-1
Concentration UV-vis g.L-1
Time (min)
0.97
0.98
0.99
1.00
1.01
0
50
100
150

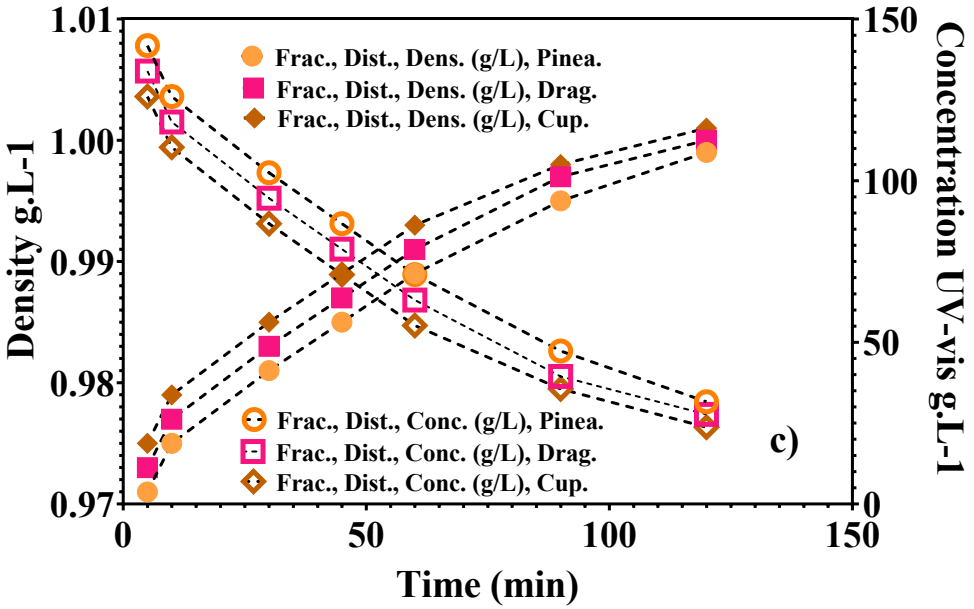


Figure 3: Temporal evolution of the concentration and purity of ethanol obtained by differential and fractional distillation from pineapple, pitaya, and cupuaçu: (a) ethanol calibration curve by UV-Vis (575 nm); ethanol concentration determined by UV-Vis (% v/v and g L^{-1}) and density of distillates determined by pycnometry (20 °C): (b) Differential Distillation and (c) Fractional Distillation. The UV-Vis data quantify the ethanol content, while the density reflects the overall composition of the ethanol-water mixture, allowing the evaluation of separation efficiency as a function of the distillation method.

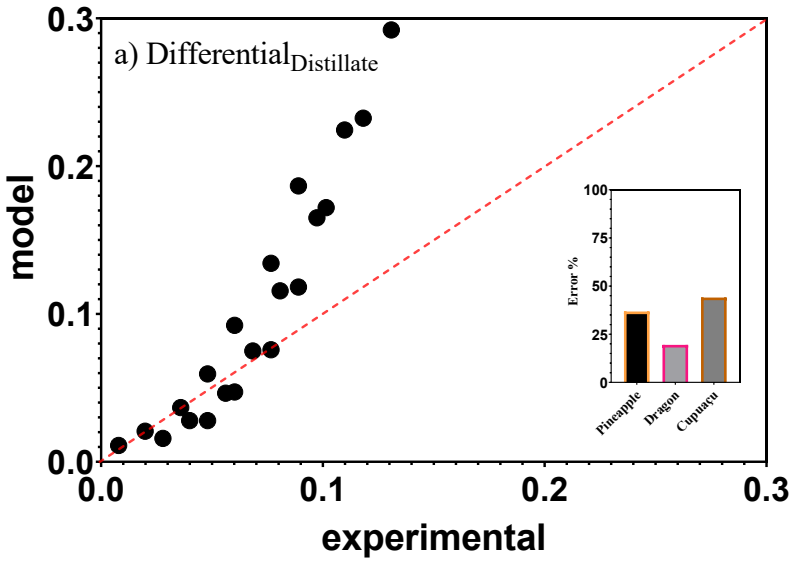
Figure 3 integrates UV–Vis quantification and density measurements to evaluate ethanol concentration evolution during distillation. Fractional distillation consistently achieved higher initial ethanol concentrations (16–18% v/v) compared to differential distillation (Caputi, A. et al., 1968).

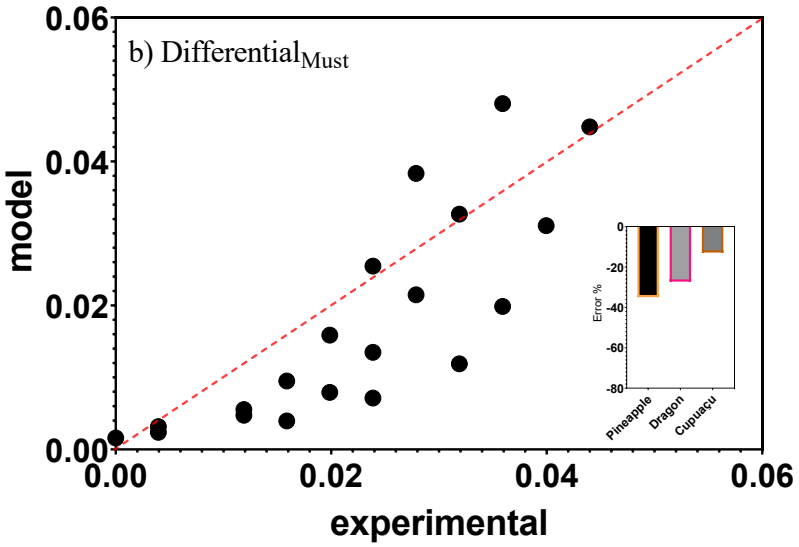
In differential distillation, the absence of reflux results in a continuously changing boiler composition, consistent with Rayleigh behavior. As distillation proceeds, ethanol concentration in the vapor rapidly declines due to progressive depletion in the liquid phase. This behavior is characteristic of a system operating with approximately one effective equilibrium stage (Seader, J. D. et al., 2011).

Conversely, fractional distillation introduces internal reflux, increasing vapor–liquid contact and enabling multiple effective equilibrium stages. This leads to higher enrichment of ethanol in early fractions and improved separation efficiency (Smith, B. D., 1963).

Density measurements corroborate UV–Vis results. Lower density values in early fractional fractions indicate higher ethanol purity, while higher densities in differential distillation reflect greater water entrainment. The agreement between independent analytical methods strengthens the reliability of the separation analysis (Nielsen, S. S., 2017).

3.4 Model Validation: Mass Balance and Separation Performance





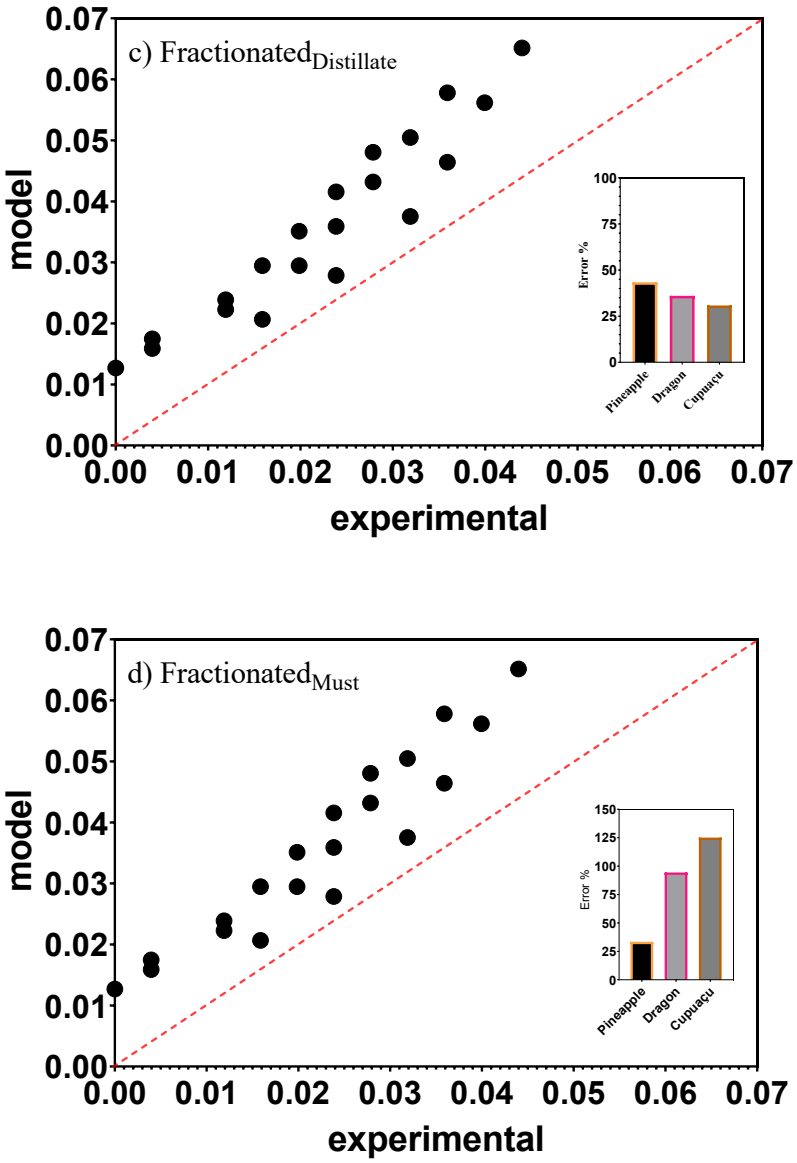
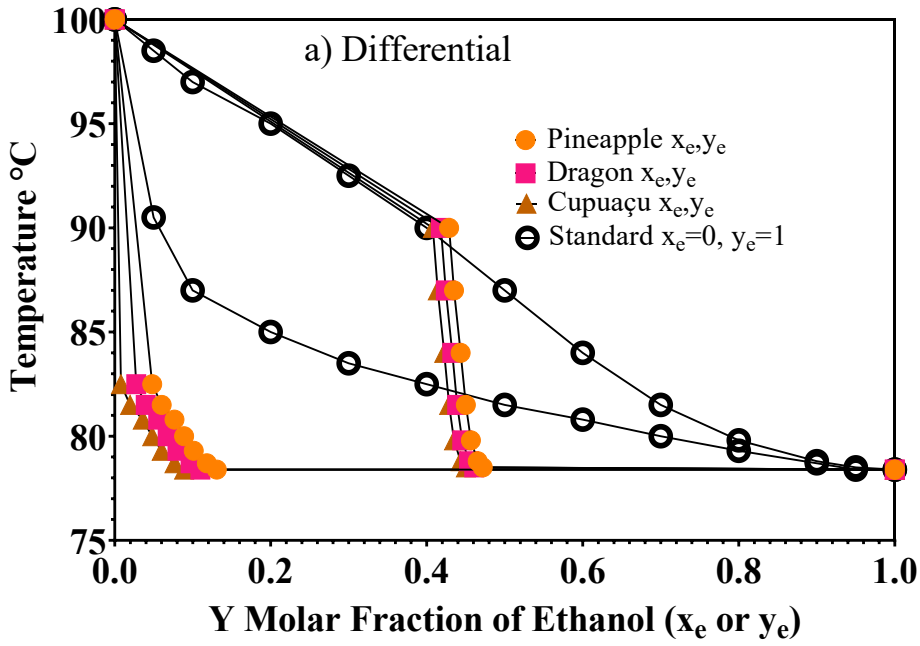


Figure 4: Comparison between experimental data obtained by density (pycnometry) and modeled values for differential and fractional distillation: (a) mass fraction of ethanol in the liquid phase (x) – differential distillation; (b) mass fraction of ethanol in the vapor/distillate phase (y) – differential distillation; (c) mass fraction of ethanol in the liquid phase (x) – fractional distillation; (d) mass fraction of ethanol in the vapor/distillate phase (y) – fractional distillation, highlighting the greater efficiency of separation and purification of ethanol in the presence of reflux.

Figure 4 compares experimental mass fraction data (x, y) obtained by density with predictions from Rayleigh-based modeling (Eq. 6) and reflux-modified balance (Eq. 14). In differential distillation, experimental points closely follow the expected monotonic

decline in ethanol composition, though deviations increase at longer times due to non-idealities, matrix complexity, and possible minor volatile interactions (Kister, H. Z., 1992). The model captures global trends but assumes ideal binary behavior and perfect equilibrium, which may not fully represent real fruit-based systems. In fractional distillation, experimental vapor-phase compositions remain significantly higher than liquid-phase compositions during early stages, confirming enhanced enrichment due to reflux (Green & Southard, 2019). The model incorporating reflux ratio provides better agreement with experimental data, validating the influence of internal liquid return on separation efficiency. The stronger depletion of ethanol in the boiler during fractional distillation confirms more effective ethanol removal and higher purification efficiency (Poling, B. E. et al., 2001).

3.5 Liquid–Vapor Equilibrium (LVE) Behavior and Thermodynamic Implications



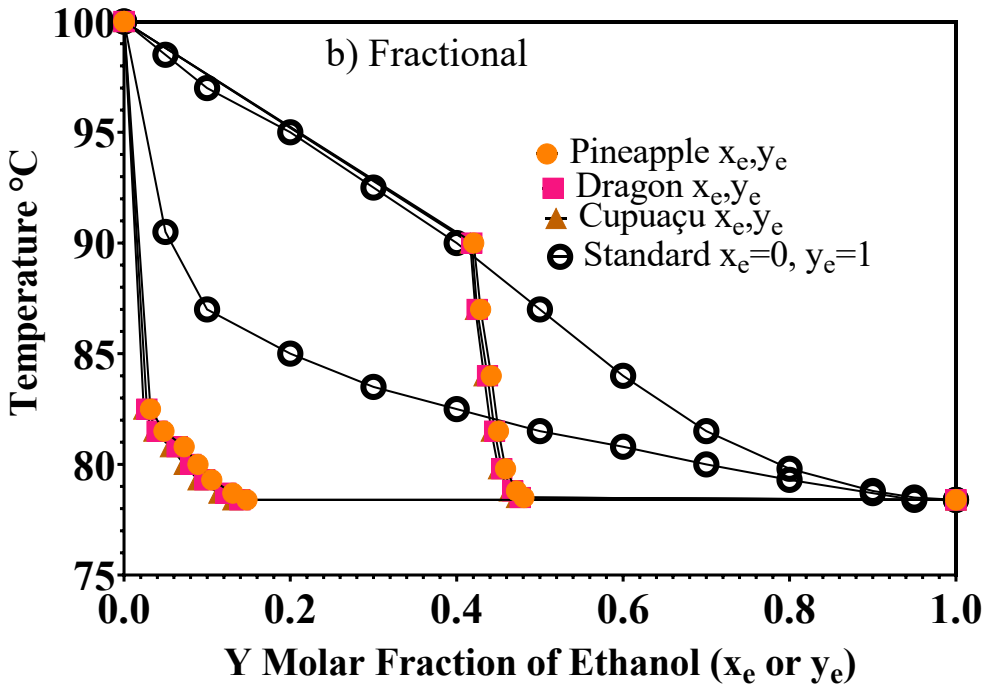


Figure 5: Liquid-vapor equilibrium (LVE) of the ethanol-water system as a function of temperature (T–x–y). (a) Differential distillation and (b) fractional distillation, for pineapple, pitaya and cupuaçu. The curves represent bubble point (saturated liquid; $Tb \times xe$) and dew point (saturated vapor; $To \times ye$), obtained from experimental data (density/pycnometry) and compared with the reference curve of 100% separation efficiency (ethanol-water system).

Figure 5 presents T–x–y diagrams constructed from experimental density data and compared with theoretical equilibrium curves for the ethanol–water system.

Maximum separation efficiency occurred near 78–79 °C, corresponding to ethanol-rich boiling conditions. Fractional distillation data approach the theoretical equilibrium envelope more closely than differential data, confirming improved vapor enrichment (Seader, J. D. et al., 2011; Litébé, M. A. et al, 2025).

Pineapple-derived data points lie closer to the ideal curve, reflecting higher initial ethanol content and improved thermodynamic driving force. Cupuaçu, with lower initial ethanol concentration, exhibits greater deviation due to higher relative water content (Mtashobya, L. et al., 2025; Poling, B. E. et al., 2001; Kister, H. Z., 1992).

These results confirm that although thermodynamic equilibrium is independent of feedstock, the initial composition strongly influences how closely the system operates to ideal separation conditions (Shirvanyan, D., 2024).

3.6 McCabe–Thiele Analysis and Theoretical Stage Estimation

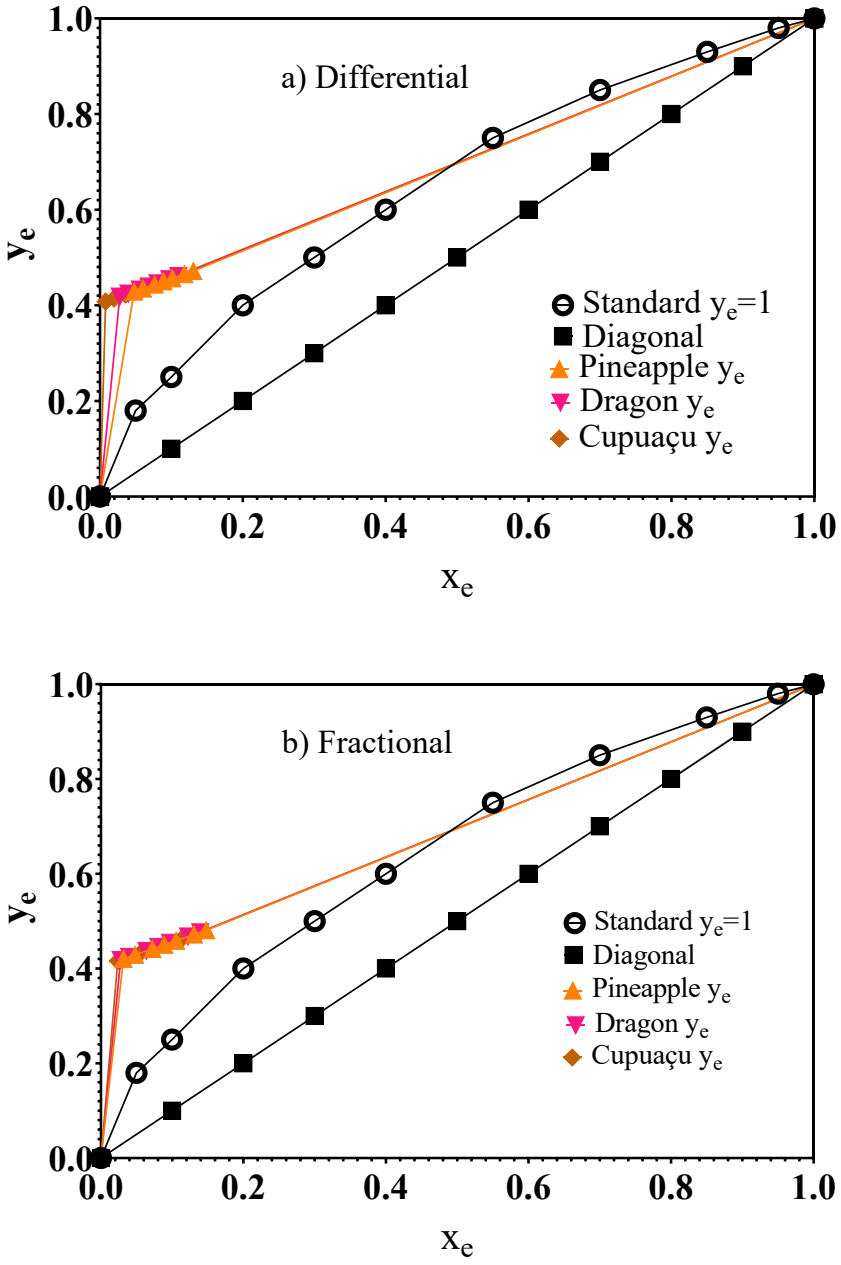
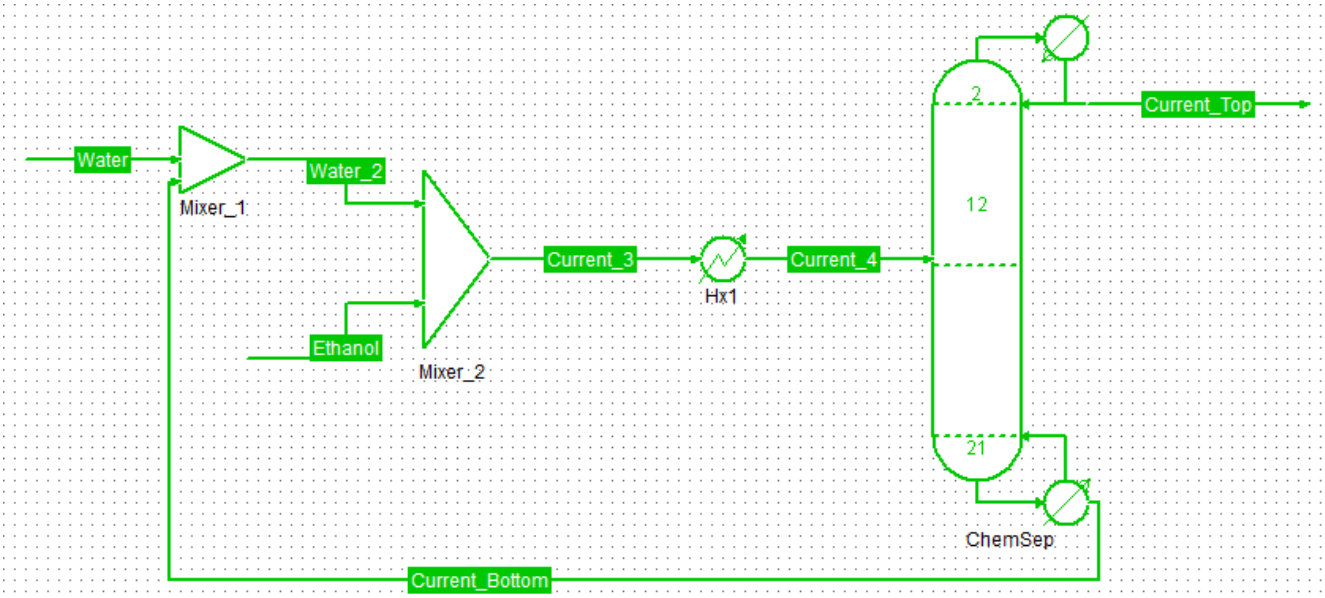


Figure 6: McCabe–Thiele (y–x) diagram for the ethanol–water system and estimate of the number of theoretical plates. (a) Differential distillation and (b) fractional distillation, with experimental points of pineapple, pitaya and cupuaçu. The diagram includes the equilibrium curve (*ye* vs. xe), the diagonal (*y*=x) and the operating lines (feed, stripping and rectification), allowing discussion of the conditions necessary to approximate the experimental behavior of the 100% efficiency standard curve and to relate the number of stages to the overall separation efficiency.

Figure 6 applies the McCabe–Thiele method to estimate the number of theoretical stages. Differential distillation shows points clustered near the diagonal (y = x), confirming minimal vapor enrichment and an effective stage number of approximately N ≈ 1(Arnautovic, Z. et al., 2022). Fractional distillation exhibits clear separation between operating lines and the diagonal, indicating multiple equilibrium stages. Estimated theoretical stages range between 4 and 6, depending on matrix composition (Zhang, R. et al., 2023; Neagu, M. et al., 2025). Pineapple achieved the highest effective stage number due to higher initial ethanol concentration. These findings confirm that separation efficiency is governed primarily by reflux and stage number rather than solely by fermentation yield (Mgeni, S. T. et al., 2024).

3.7 Process Simulation and Industrial Implications



Stream	Water	Water_2	Ethanol	Current_3	Current_4	Current_Bottom	Current_Top	Unit
Pressure	1	1	1	1	1	1	1	atm
Temperature	25	99.6042	25	99.6041	78	99.6044	78.6494	°C
Mass frac Water	1	0.997447	0	0.997446	0.997446	0.997447	0.000391293	
Mass frac Ethanol	0	0.00255321	1	0.00255378	0.00255378	0.00255321	0.999609	
Flow Ethanol	0	2222.59	0.5	2223.09	2223.09	2222.59	0.499745	ton / h
Flow Water	0.1	868285	0	868285	868285	868285	0.000195623	ton / h

Figure 7: Simulated flowchart of the pilot-scale ethanol production process from a binary ethanol-water feed, representative of fermented musts of tropical fruits.

Figure 7 presents the pilot-scale process simulation integrating mixing, heating, fractionation, and heat exchange. Simulation results indicate that: Must standardization is required to reduce feed variability; Fractionated columns with adequate reflux are

essential for industrial-scale purification; Heat integration significantly reduces global energy demand; Pineapple requires lower specific energy per unit ethanol recovered (Seader, J. D. et al., 2011; Humbird, D. et al., 2011). The results highlight that industrial feasibility depends on process integration rather than isolated fermentation performance (Mgeni, S. T. et al., 2024; Green & Southard, 2019). Tropical fruits – particularly pineapple – are technically viable feedstocks when integrated within circular bioeconomy systems utilizing agro-industrial residues.

4. Conclusion

This study demonstrates the technical feasibility of ethanol production from tropical biomass matrices – pineapple, dragon fruit, and cupuaçu – through an integrated approach combining alcoholic fermentation, distillation, and thermodynamic analysis. The initial reducing sugar content was identified as the key variable governing theoretical ethanol yield and subsequent separation performance. Pineapple exhibited the highest fermentable potential, resulting in greater ethanol concentration in the must and improved downstream efficiency. Fermentation yields ranged from 76–85% of theoretical values, consistent with complex natural substrates and typical metabolic losses. Comparative evaluation of separation strategies showed that differential distillation is limited by its single effective equilibrium stage, leading to lower ethanol enrichment. In contrast, fractional distillation significantly improved recovery and purity due to internal reflux, increasing the number of effective theoretical stages to approximately 4–6. Liquid–vapor equilibrium analysis and McCabe–Thiele diagrams confirmed that reflux ratio and stage number are the dominant parameters controlling separation efficiency. Process simulation further indicated that industrial implementation requires must standardization, adequate reflux control, and thermal integration to reduce energy demand. Overall, tropical fruit biomass – particularly pineapple – represents a promising feedstock for sustainable ethanol production within circular bioeconomy systems.

Acknowledgment

The authors gratefully acknowledge the financial support provided by the Federal Institute of Education, Science and Technology of Rondônia (IFRO) through *Edital nº 3/2025/REIT/PROPESP/IFRO* and *Edital nº 4/2025/REIT/PROPESP/IFRO*. The support

received under these institutional funding programs was essential for the development of the experimental activities, analytical procedures, and process modeling carried out in this study.

Reference

1. DIAS, M. O. S.; et al. *Integrated versus stand-alone second generation ethanol production from sugarcane bagasse and trash.* Bioresource Technology, 2012, 103, 152–161.
2. BALAT, M.; BALAT, H. *Recent trends in global production and utilization of bio-ethanol fuel.* Applied Energy, 2009, 86, 2273–2282.
3. KIM, S.; DALE, B. E. *Global potential bioethanol production from wasted crops and crop residues.* Biomass and Bioenergy, 2004, 26, 361–375.
4. GNANSOUNOU, E.; DAURIAT, A. *Techno-economic analysis of lignocellulosic ethanol: A review.* Bioresource Technology, 2010, 101, 4980–4991.
5. KISS, A. A.; et al. *Process intensification in bioethanol production – An overview.* Chemical Engineering and Processing, 2013, 65, 1–15.
6. LUYBEN, W. L. *Design and control of conventional and reactive distillation processes.* Ind. & Eng. Chem. Res., 2011, 50, 11481–11498.
7. TOWLER, G.; SINNOTT, R. *Chemical Engineering Design.* Elsevier, 2013.
8. BIEGLER, L. T.; GROSSMANN, I. E.; WESTERBERG, A. W. *Systematic methods of chemical process design.* Prentice Hall, 1997.
9. CARDONA, C. A.; SÁNCHEZ, O. J. *Fuel ethanol production: Process design trends and integration.* Bioresource Technology, 2007, 98, 2415–2457.
10. YAWS, C. L. *Thermophysical properties of chemicals and hydrocarbons.* Elsevier, 2008.
11. CAPUTI, A.; UEDA, M.; BROWN, T. Spectrophotometric determination of ethanol in wine. American Journal of Enology and Viticulture, 1968, 19, 160–165.
12. RAMSAROOP, R. E.; SAUNDERS, S. R. Sugar composition of pineapple (Ananas comosus) at different stages of maturity. Journal of Food Composition and Analysis, 25, 134–140, 2012.
13. WU, L. et al. Physicochemical properties and sugar profile of pitaya (Hylocereus spp.). Food Chemistry, 135, 2517–2521, 2012.

14. WALKER, G. M.; STEWART, G. G. Saccharomyces cerevisiae in the production of fermented beverages. Beverages, 2, 30, 2016.
15. CORTEZ, L. A. B.; LORA, E. E. S.; GÓMEZ, E. O. Biocombustíveis no Brasil: fundamentos, aplicações e perspectivas. Campinas: UNICAMP, 2008.
16. MUSSATTO, S. I. et al. Production of bioethanol from agro-industrial residues. Bioresource Technology, 101, 4162–4175, 2010.
17. BAI, F. W.; ANDERSON, W. A.; MOO-YOUNG, M. Ethanol fermentation technologies from sugar and starch feedstocks. Biotechnology Advances, 26, 89–105, 2008.
18. CAPUTI, A.; UEDA, M.; BROWN, T. Spectrophotometric determination of ethanol in wine. American Journal of Enology and Viticulture, 19, 160–165, 1968.
19. SEADER, J. D.; HENLEY, E. J.; ROPER, D. K. *Separation Process Principles: Chemical and Biochemical Operations*. 3rd ed. New York: Wiley, 2011.
20. SMITH, B. D. Design of Equilibrium Stage Processes. New York: McGraw-Hill, 1963.
21. NIELSEN, S. S. Food Analysis. 5th ed. New York: Springer, 2017.
22. GREEN, D. W.; SOUTHARD, M. Z. Perry's Chemical Engineers' Handbook. 9th ed. New York: McGraw-Hill, 2019.
23. POLING, B. E.; PRAUSNITZ, J. M.; O'CONNELL, J. P. *The Properties of Gases and Liquids*. 5th ed. New York: McGraw-Hill, 2001.
24. KISTER, H. Z. Distillation design and control using vapor and liquid traffic. *Industrial & Engineering Chemistry Research*, 31, 1249–1260, 1992.
25. LITÉBÉ, M. A.; NDZIÉ, J. P.; NDZIÉ, E. J.; NDZIÉ, A. M. Production of bioethanol from tropical fruit wastes (pineapple, banana and papaya): fermentation performance and fuel potential. Journal of Green Economy and Environment, 2025, 5, 1–12.
26. MTASHOBYA, L.; MGHANGA, J.; MWAKITALU, E.; KIMARO, D. Bioethanol production from fruit waste juices using bakery yeast. *Materials for Renewable and Sustainable Energy*, 2025, *14*, 6.
27. SHIRVANYAN, D.; HARUTYUNYAN, H.; VARDANYAN, Z.; STEPANYAN, A. Biomass and bioethanol production from pretreated mixed fruit peel hydrolysate using Saccharomyces cerevisiae strains. BMC Biotechnology, 2024, 24, 92.

28. ARNAUTOVIC, Z.; WEITH, T.; HEBERLE, F.; BRÜGGEMANN, D. Isobaric vapor-liquid equilibrium for ethanol/water and binary linear siloxane mixtures at 100 kPa. Fluid Phase Equilibria, v. 556, art. 113371, 2022.
29. ZHANG, R.; HE, Y.; YANG, L.; ZHENG, K.; XIA, M.; LI, G.; MENG, X.; XU, C. Systematic study of energy-saving bioethanol distillation process with sidestreams: Design and control. Energy Conversion and Management, v. 297, art. 117736, 2023.
30. NEAGU, M.; PRICOP-NICOLAE, M. Azeotropic and Extractive Distillation for Bio-Ethanol Dehydration: Process Design, Simulation, and Cost Analysis. Processes, v. 13, n. 11, art. 3634, 2025.
31. MGENI, S. T.; MERO, H. R.; MTASHOBYA, L. A.; EMMANUEL, J. K. The prospect of fruit wastes in bioethanol production: A review. Heliyon, v. 10, n. 19, e38776, 2024.
32. HUMBIRD, D.; DAVIS, R.; TAO, L.; et al. Process design and economics for the production of fuel ethanol from lignocellulosic biomass. National Renewable Energy Laboratory (NREL), Technical Report NREL/TP-5100-47764, 2011.